Statistical properties of random scattering matrices

Petr Šeba,[1] Karol Życzkowski,[2] and Jakub Zakrzewski[2,3]

[1]*Nuclear Physics Institute, Czech Academy of Sciences, 250 68 Řež near Prague, Czech Republic*
[2]*Instytut Fizyki Mariana Smoluchowskiego, Uniwersytet Jagielloński, ul. Reymonta 4, 30-059 Kraków, Poland*
[3]*Laboratoire Kastler–Brossel, Université Pierre et Marie Curie, T12, E1, 4 place Jussieu, 75272 Paris Cedex 05, France*

We discuss the statistical properties of eigenphases of S matrices in random models simulating quantum systems that exhibit chaotic scattering classically. The energy dependence of the eigenphases is investigated and the corresponding velocity and curvature distributions are obtained both theoretically and numerically. A simple formula describing the velocity distribution (and hence the distribution of the Wigner time delay) is derived that is capable of explaining the algebraic tail of the time delay distribution observed recently in microwave experiments. A dependence of the eigenphases on other external parameters is also discussed. We show that in the semiclassical limit (large number of channels) the curvature distribution of S-matrix eigenphases is the same as that corresponding to the curvature distribution of the underlying Hamiltonian and is given by the generalized Cauchy distribution. [S1063-651X(96)03209-6]

I. INTRODUCTION

Quantum chaotic scattering has been discussed for a number of years [1,2]. It may occur in a variety of different physical situations from atoms and nuclei to disordered mesoscopic devices or microwave cavities. The schematic model of the system is presented in Fig. 1. The cavity (internal region) is coupled to the outside world by leads. The characterictics of the internal motion manifest themselves obviously in the properties of the S matrix. This is seen directly using the Hamiltonian approach to the scattering [3].

Consider a simple Hamiltonian with the Hilbert space spanned by N discrete states $|k\rangle$ and M continua $|c,E\rangle$:

$$H = \sum_{k=1}^{N} E_k |k\rangle\langle k| + \sum_{c=1}^{M} \int dE\, E |c,E\rangle\langle c,E|$$
$$+ g \sum_{c=1}^{M} \sum_{k=1}^{N} \int dE [W_{kc}(E)|k\rangle\langle c,E| + \text{H.c.}]. \quad (1.1)$$
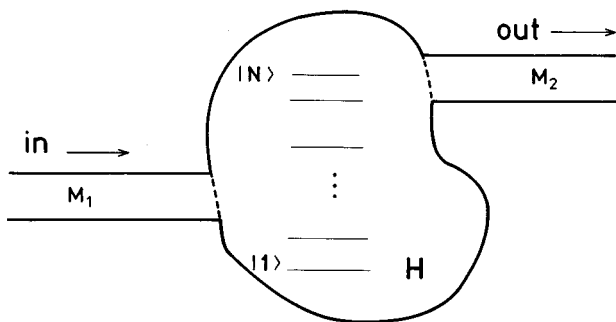

FIG. 1. Scheme of the scattering system. A system containing N bounded states and described by a Hamiltonian H is coupled via matrices W and $W^\dagger$ to two waveguides with M_1 and M_2 open channels. The scattering in the system is thus characterized by an $M \times M$ matrix S, where $M = M_1 + M_2$.

Note that no continuum-continuum coupling is permitted in the model. The bound-continuum coupling is characterized by coupling constant g and the energy dependent matrix $W_{kc}(E)$, where it is assumed that the columns of W are normalized to unity. If W depends only weakly on the energy, the corresponding unitary $M \times M$ matrix S may be expressed as [3,4]

$$S_{cc'}(E) = \delta_{cc'} - 2g^2 i \sum_{kl} W_{ck}(E)\left(\frac{1}{E-\mathcal{H}}\right)_{kl} W_{lc'}(E),$$
$$(1.2)$$

where $\mathcal{H}$ is the effective Hamiltonian describing the motion within the bound subspace after eliminating the continua in a Markov approximation. In an arbitrary basis spanning the bound subspace it takes the form

$$\mathcal{H}_{kl} = H_{kl} - ig^2 \sum_{c=1}^{M} W_{kc} W_{cl}. \quad (1.3)$$

The question may be posed whether, for generic systems, there is a unique relation between S-matrix properties and the type of motion inside the cavity. One way to address this issue is via the semiclassical theory [1], which seems, however, to be limited to a large number of channels, M. On the other hand, in recent experiments on scattering in microstructures [5,6] M can be of the order of unity.

A second possible way is a stochastic approach in which the Hamiltonian H and the coupling matrix W [2] are modeled by random matrices. A subsequent averaging over different realizations of H (typically for fixed W) yields statistical predictions concerning fluctuations of physical quantities of interest. One hopes, extending the conjecture which has been quite useful for bounded chaotic systems [7], that the properties of fluctuations are universal. For bounded, autonomous, classically chaotic systems, depending on their symmetries, the statistical spectral fluctuations are, generically, well represented by the corresponding quantities ob-

tained from Gaussian orthogonal (GOE), unitary (GUE), or symplectic (GSE) ensembles of random matrices [8].

Assuming that H matrices are drawn from one of these ensembles and making similar assumptions on the coupling matrix W, one is forced to ask what are the properties of the ensemble of S matrices. A partial answer has been obtained by Lewenkopf and Weidenmüller [2]: if H belongs to GOE and the channels are equivalent (see below) the S matrix belongs to COE provided the coupling constant g is equal to unity. This result has been recently generalized to all three universality classes by Brouwer [9] for arbitrary g. Brouwer found that the S matrices, Eq. (1.2), conform with generalized orthogonal (GCOE) and unitary (GCUE) circular ensembles [10] which reduce to circular ensembles of Dyson (COE, CUE) [11], when the coupling to the continuum becomes ideal.

Brouwer's result provides a direct link with another popular, random matrix theory based approach in which one draws directly S matrices, or transmission matrices, from an appropriate random matrix ensemble [10,12,13]. The Hamiltonian approach is, in a sense, more general since it allows for calculation of time delays and energy-correlation averages, while the ensemble of S matrices is energy independent. On the other hand, one is frequently interested in single-point with respect to energy statistical measures. Those may be directly accessed from the ensemble of S matrices. In such a way one may obtain, e.g., the universal conductance fluctuations [14] from the random matrix model [12].

The study of mesoscopic devices points out that the random matrix approach has its limitations, e.g., the fluctuations may become dependent on the length of the device [15]. It is still an open question what the limits are of the universality. We do not address this problem here, rather we want to study, within the random model, the generic properties of S matrices dependent on some parameter. In this way we extend recent intensive studies of the statistical properties of bound systems dependent on the external parameters [16–19].

For parameter independent Hamiltonians statistical properties are generically universal once the mean level spacing Δ is known. Parametric measures reveal a similar universality; in addition to unfolding the energy levels one has to unfold the parameter dependence [16,17]. On the other hand, much less is known about the parametric behavior of scattering systems. The two-point correlation function for the S matrix with respect to an external parameter was derived recently by Macêdo [20]. The conductance fluctuations in the presence of the magnetic field induced time-reversal symmetry breaking have been studied by Pluhař *et al.* [21]. The semiclassical properties of the so-called Wigner time delay have been discussed by Jalabert and Pichard [15]. Obviously, even in the absence of the external parameter the S matrix is energy dependent — the corresponding correlation function was obtained in [2].

Instead of investigating the S matrix elements we focus on the properties of the corresponding eigenphases (phase shifts). Some important dynamical features of the system (for instance the time delay inside the interaction region) can be easily expressed using the derivatives of S-matrix eigenphases. Being directly accessible in experiments, statistical properties of phase shifts deserve a detailed study. The nearest-neighbor spacing distribution has been discussed in Refs. [22,23]. As mentioned above, we consider here parametric dependence of phase shifts.

The paper is organized as follows. The analytic results concerning the distribution of velocities (i.e., first derivatives of eigenphases with respect to energy or other external parameter), also referred to as slopes, are discussed in Sec. II. Here we discuss also briefly the distribution of the second derivatives, i.e., the curvatures of the eigenphases. These predictions are tested against numerical results obtained from simulations based on Eqs. (1.1) and (1.2) (and their generalization allowing for the presence of some external parameter) in Sec. III. For systems dependent on the external parameter one may also construct directly circular ensembles of scattering matrices. The corresponding results are presented in Sec. IV.

II. PARAMETRIC HAMILTONIAN APPROACH TO S MATRIX

Consider the unitary matrix S defined by Eqs. (1.2) and (1.3). To discuss properties of the eigenphases of the S matrix it is convenient to rewrite Eq. (1.2) as

$$S(E) = \frac{1+iA}{1-iA}, \qquad (2.1)$$

with A given by

$$A = g^2 W^\dagger \frac{1}{E-H} W. \qquad (2.2)$$

Eigenphases s_m of the unitary matrix S are related to eigenvalues a_m of the $M \times M$ Hermitian matrix A by [9]

$$s_m = 2 \arctan(a_m), \quad m = 1, \ldots, M. \qquad (2.3)$$

Since s_m is a function of a_m, the statistical properties of s_m and a_m are identical after unfolding. In the semiclassical limit (large M) it has been shown [9] that A belongs to the same ensemble as H. This implies that the statistical properties (level spacing, number variance, etc.) of s_m are identical with those of the eigenvalues of H. Moreover, the relation (2.3) is useful when discussing the parametric dependence of s_m.

To see how it works consider the slopes of the eigenphases with respect to the energy E. They have a direct physical significance as time delays associated with the corresponding phase shifts (see, e.g., [15]) while the average slope is just the celebrated Wigner time delay.

The eigenequation for a_m,

$$A|f_m\rangle g^2 W^\dagger \frac{1}{E-H} W |f_m\rangle = a_m |f_m\rangle, \qquad (2.4)$$

is equivalent to

$$\left(H+\frac{g^2}{a_m}WW^\dagger\right)|h_m\rangle=E|h_m\rangle \tag{2.5}$$

with $|f_m\rangle$ and $|h_m\rangle$ related by $|h_m\rangle=(1/E-H)W|f_m\rangle$. Note that the $N\times N$ eigenvalue problem Eq. (2.5) has, for fixed E, only M nontrivial solutions a_m and corresponding eigenvectors $|h_m\rangle$. This is related to the fact that $M-N$ eigenvalues of $WW^\dagger$ vanish. Differentiating Eq. (2.5) with respect to E for nontrivial a_m one gets

$$\frac{g^2}{a_m^2}\frac{da_m}{dE}\langle h_m|WW^\dagger|h_m\rangle=\langle h_m|h_m\rangle \tag{2.6}$$

We shall assume from now on that $|h_m\rangle$ are normalized to unity.

Using the relation (2.3) between s_m and a_m, we express the inverse time delay as

$$u_m=\tau_m^{-1}=\frac{1}{ds_m/dE}=\frac{1+a_m^2}{da_m/dE}. \tag{2.7}$$

Thus eliminating the derivative via Eq. (2.6) we obtain

$$u_m=g^2\langle h_m|WW^\dagger|h_m\rangle+g^2\frac{\langle h_m|WW^\dagger|h_m\rangle}{a_m^2}. \tag{2.8}$$

But it follows from Eq. (2.4) and the relation between $|f_m\rangle$ and $|h_m\rangle$ that the second term on the right-hand side above is proportional to the norm $\langle f_m|f_m\rangle$. Thus finally we get

$$u_m=g^2\langle h_m|WW^\dagger|h_m\rangle+\langle f_m|f_m\rangle/g^2. \tag{2.9}$$

Equation (2.9) indicates that the distribution of inverse time delays is related to the norms appearing on its right-hand side (rhs). Having in mind that $\langle h_m|WW^\dagger|h_m\rangle$ is a sum of M terms,

$$\langle h_m|WW^\dagger|h_m\rangle=|\langle h_m|w_1\rangle|^2+\cdots+|\langle h_m|w_M\rangle|^2, \tag{2.10}$$

where w_k, $k=1,\ldots,M$, are vectors describing the coupling to the channel k, we can estimate the distribution of the matrix element $\langle h_m|WW^\dagger|h_m\rangle$ by a χ^2 distribution with M degrees of freedom in the GOE case and $2M$ degrees of freedom in the GUE case, respectively. On the other hand, $\langle f_m|f_m\rangle$ has a χ^2 distribution with 1 (GOE case) or 2 (GUE case) degrees of freedom. Assuming the two terms on the rhs of Eq. (2.9) to be independent, we obtain the distribution $P(u)$ by convolution of two χ_ν^2 distributions with a different number of degrees of freedom and different means. The result can be expressed in terms of the confluent hypergeometric function $_1F_1(a;c;x)$, sometimes called the Kummer function [24]. Changing the variable to $\tau=1/u$ we obtain the distribution of time delays,

$$P(\tau)=\frac{\exp\left[-\dfrac{g^2}{\tau}\right]{}_1F_1\left(\dfrac{M\beta}{2};\dfrac{(M+1)\beta}{2};(g^2-g^{-2})\dfrac{1}{\tau}\right)}{g^{\beta(M-1)}\Gamma\left(\dfrac{\beta(M+1)}{2}\right)\tau^{\beta\frac{M+1}{2}+1}}, \tag{2.11}$$
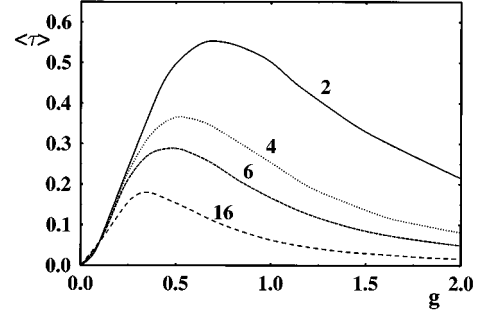

FIG. 2. Dependence of the mean time delay $\langle\tau\rangle$ on the coupling constant g for $\beta=2$. Number of channels M labels each curve.

where $\beta=1,2$ for orthogonal and unitary ensembles, respectively.

Figure 2 shows the mean time delay $\langle\tau\rangle$ as a function of g obtained by integration of the above distribution for $\beta=2$ and $M=2,4,6$, and 16. In general, mean time delay decreases with M. Moreover, the value of the coupling constant g_m, for which the mean delay time is maximal, decreases with the number of channels. In both limiting cases $g\to0$ and $g\to\infty$ the mean time delay tends to zero, but the physical meaning of this fact is different. In the former case the coupling is so weak that the scattered wave is not affected by the bound system H. In the latter case very strong coupling causes the scattering to occur almost instantaneously.

Formula (2.11) simplifies in the special case $g=1$. Then the inverse time delays are distributed according to χ^2 distribution with $\beta(M+1)$ degrees of freedom and the mean $\langle u\rangle=\beta(M+1)/2$. The time delay distribution $P(\tau)$ is then

$$P(\tau)=\frac{1}{\Gamma\left(\dfrac{\beta(M+1)}{2}\right)}\tau^{-\beta\frac{M+1}{2}-1}e^{-1/\tau}, \tag{2.12}$$

with the mean time delay

$$\langle\tau\rangle=2/[\beta(M+1)-2]. \tag{2.13}$$

For a large number of channels M the χ^2 distribution can be approximated by a Gaussian with the variance equal to the mean $\langle u\rangle$. Thus for M large

$$P(\tau)=\frac{2\alpha}{\sqrt{\pi}\tau^2}\exp\{-\alpha^2(2/\tau-2/\tau_0)^2\}, \tag{2.14}$$

where $\alpha^2=1/[4\beta(M+1)]$ and $\tau_0=2/\beta(M+1)$.

The algebraic tail (for τ large) obtained for the time delay distribution [Eqs. (2.11)–(2.12)] is characterized solely by the number of open channels, M, and the universality class (orthogonal or unitary) of a system studied. Thus its origin is purely quantum, since the algebraic tail disappears in the semiclassical limit, $M\to\infty$. Looking back at the derivation of the time-delay distribution it becomes apparent that the algebraic tail originates from the properties of the eigenvectors, $|h_m\rangle$, of the Hamiltonian problem, Eq. (2.5), or rather their products with vectors describing the coupling to the continuum. The statistical properties of the latter are known

from the random matrix theory [27]. Clearly the result obtained is valid only for chaotic systems whose statistical properties are well approximated by the random approach. In particular, since eigenvector properties change for integrable or mixed systems, a similar change, violating Eq. (2.11), is expected for time delay distribution if the internal dynamics becomes classically not fully chaotic. Discussion of such a situation is beyond the scope of the present study.

Consider now the case when the Hamiltonian $H = H(x)$ depends on some external parameter x and investigate the properties of $s_m(x)$ keeping the energy E fixed.

Equation (2.5), putting explicitly the x dependence, takes the following form:

$$\left(H(x) + \frac{g^2}{a_m(x)} \, WW^\dagger \right)|h_m(x)\rangle = E|h_m(x)\rangle, \quad (2.15)$$

and may be viewed as an eigenvalue equation for eigenvalues $E_n(a,x)$ of the matrix $H(x) + g^2/a \, WW^\dagger$, defined for any real parameter a. Then Eq. (2.15) is equivalent to a set of implicit equations

$$E_n(a,x) = E; \quad n = 1, 2, \ldots, N \quad (2.16)$$

for an unknown $a(x)$. Again due to the positivity of $WW^\dagger$, Eq. (2.16) has at most one solution $a_m(x)$ for each n with the total number of all possible solutions being equal to M. Moreover, from Eq. (2.16) follows

$$\frac{da_m(x)}{dx} = \frac{\partial E_m(a,x)}{\partial x} \, \frac{a_m^2}{g^2\langle h_m|WW^\dagger|h_m\rangle}, \quad (2.17)$$

where E_m denotes those eigenvalues for which Eq. (2.16) has a nontrivial solution. Combining Eqs. (2.17) and (2.3) together with Eq. (2.6) yields simply

$$v_m = \frac{d}{dx} s_m = \tau_m \frac{\partial E_m}{\partial x} \quad (2.18)$$

providing the connection between the slope of the eigenphase with respect to external parameter x, the corresponding time delay, and the slope of the *Hermitian* eigenvalue problem Eq. (2.15). The generic distribution of slopes for Hermitian random matrices is Gaussian-like [17,18]. Thus the eigenphases slope distribution $P(v)$ may be obtained as a simple integral of the Gaussian and $P(\tau)$ given by Eq. (2.12) (we consider the critical coupling $g = 1$ case only):

$$P(v) = \frac{1}{\sqrt{2\pi}} \int_0^\infty P(\tau) \exp\left(-\frac{v^2}{2\tau^2}\right) \frac{d\tau}{\tau}, \quad (2.19)$$

under the assumption that appropriate unfolding of the parameter, x, has been made [17,18]. The integral in (2.19) yields [25]

$$P(v) = \frac{\beta(M+1)}{\sqrt{8\pi} v^{\beta(M+1)/2+1}} \mathcal{D}_{-\beta(M+1)/2-1}(1/v), \quad (2.20)$$

where $\mathcal{D}_p(z)$ is a shorthand notation for the product of the parabolic cylinder function, $D_p(z)$ [25], with the exponential

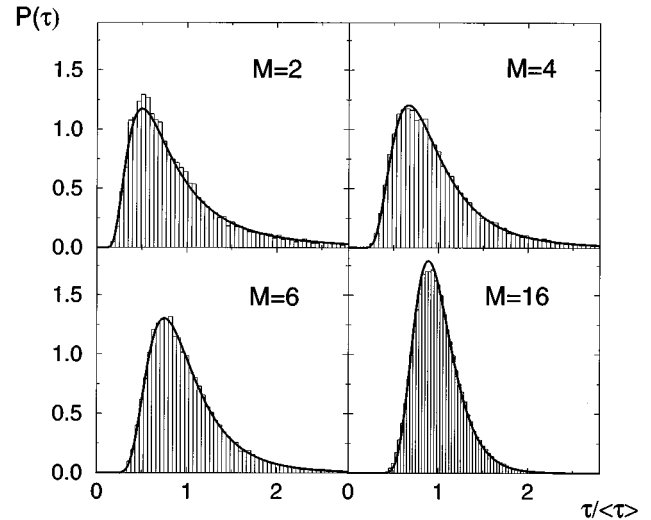$$\mathcal{D}_p(z) = \exp(z^2/4) D_p(z). \quad (2.21)$$

FIG. 3. Time delay distributions $P(\tau)$ for GUE internal dynamics, $g = 1$, and for a different number of open channels, M, as indicated in the figure. The numerical data (histograms) and the theoretical distributions (solid lines), $P_2(\tau)$, Eq. (2.12) are presented as a function of $\tau/\langle\tau\rangle$ to facilitate comparison of distribution shape for different M. According to Eq. (2.13), $\langle\tau\rangle$ is inversely proportional to M.

Using the series representation of $\mathcal{D}_p(z)$ for small z one easily verifies that the large $|v|$ tail of $P(v)$ decays algebraically as $P(v) \propto 1/|v|^{\beta(M+1)/2+1}$. The asymptotic form of $\mathcal{D}_p(z) = z^p[1 + O(z^{-2})]$ [25] valid for large z yields regular behavior of $P(v)$ for $|v|$ small.

Let us recall that the distribution of level slopes with respect to an external parameter, x, for a bounded generic system is Gaussian [17,18]. It is remarkable that the corresponding slope distibution for the eigenphases of the S matrix reveals the algebraic tails. As we shall demonstrate in the numerical example below, for large M the algebraic tail asymptotic form appears for very large $|v|$ only, while the center of the distribution resembles a Gaussian. One may verify, using the asymptotic form of $P(\tau)$ given by Eq. (2.14), that the Gaussian distribution for $P(v)$ is recovered in the $M \to \infty$ limit.

A similar analysis can be carried out also for curvature distribution. In the limit of large M it can be shown in such a way that the curvature distribution tends to the generalized Cauchy one, as for the bounded systems [18].

III. NUMERICAL RESULTS—HAMILTONIAN APPROACH

The numerical results have been obtained by a direct diagonalization of the S matrices generated following random matrix theory. A given S matrix is defined by providing the internal dynamics Hamiltonian, H, and the matrix W describing the coupling to the continuum. Consider the time-reversal invariant case (GOE) for simplicity. A given H matrix is constructed [7] by filling the Hamiltonian matrix with Gaussian distributed random numbers of zero mean and a given variance, the diagonal elements having twice the variance of the nondiagonal elements. The $N \times M$ matrix W is built from arbitrarily chosen M eigenvectors of $N \times N$ auxiliary matrix H' (H' is independent of H but belongs to the
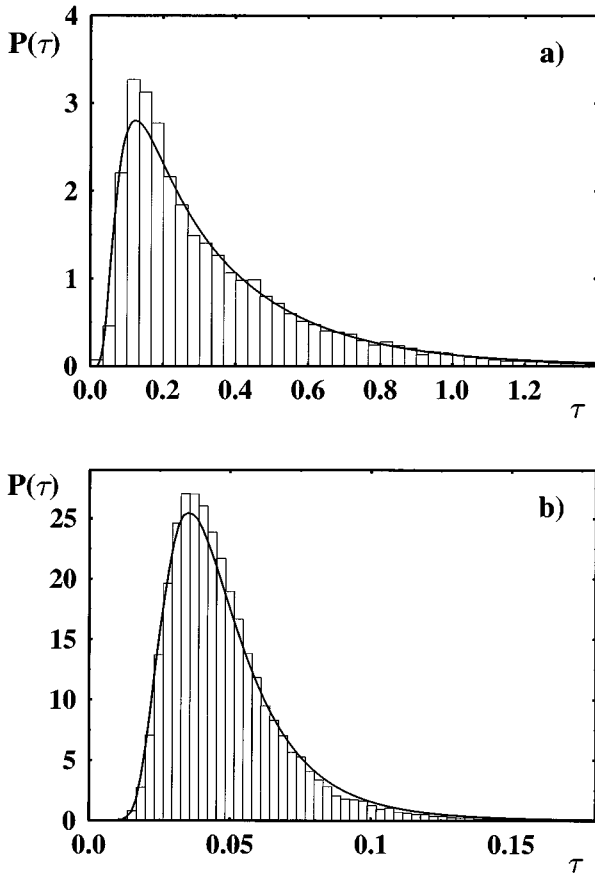
FIG. 4. Time delay distributions $P(\tau)$ for GUE internal dynamics and $g \neq 1$: (a) $g = 0.5$, $M = 4$; (b) $g = 2.0$, $M = 6$. Solid line represents the theoretical prediction as given by Eq. (2.11).

FIG. 5. Time delay distribution $P(\tau)$ for time reversal invariant (GOE) internal dynamics, $g = 1$, and for a different number of open channels, M, as indicated in the figure. The numerical data (histograms) are compared with both the analytical prediction, Eq. (2.12) (dashed lines), and the corrected prediction, Eq. (3.1) (represented by a solid line).

same ensemble, e.g., GOE). The vectors are normalized, so the strength of the coupling is determined by the parameter g. A diagonalization of $S(E)$ yields then the set of M eigenphases.

The derivatives with respect to energy E are then obtained by a finite difference method, from two sets of eigenphases obtained at E and $E + \delta E$. The procedure is repeated by taking different, independent realizations of the internal Hamiltonian, H, and keeping the coupling matrix W fixed [2].

We discuss the numerical results obtained for the slopes with respect to the energy, E, first. As discussed above, they are directly related to possible time delays in the scattering process and are, therefore, of particular interest. The time delay distributions $P(\tau)$ obtained numerically by diagonalizing the S (1.2) for various numbers of channels M and $g = 1$ in the GUE case are presented in Fig. 3 and compared with the formula (2.12). The dimension of the internal Hamiltonian was taken $N = 100$, energy E was set to zero, and the data were obtained from 15 000 generated S matrices. Fine agreement of the numerical results with the formula (2.12) does not depend on the energy and the number of eigenstates, provided $N \gg M$ and E is not too large. Figure 4 shows a comparison of the distribution $P(\tau)$ obtained for $g \neq 1$ and the formula (2.11). Again the agreement is quite satisfactory.

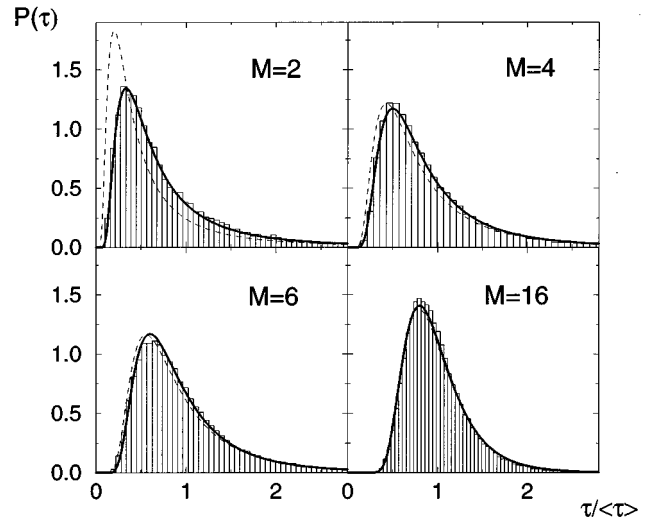Analogous results for the GOE case and $g = 1$ are plotted in Fig. 5 (dashed line). The agreement with the prediction

(2.12) is not so nice as in the GUE case. Especially for small M a discrepancy is significant. Importantly, it may be removed when we use the formula (2.12) with *one additional degree of freedom*, i.e.,

$$\widetilde{P}(\tau) = \frac{1}{\Gamma\left(\dfrac{M+2}{2}\right)} \tau^{-\frac{M}{2}-2} e^{-\frac{1}{\tau}}. \tag{3.1}$$

The corresponding average time delay is given by Eq. (2.13) with $\beta = 1$ and $M \to M + 1$ substitutions. We are not able to give a plausible explanation for this additive degree of freedom. The numerical results demonstrate clearly, however, that it is superior to Eq. (2.12) and leads to an excellent agreement with the numerical data — see Fig. 5.

Formula (3.1) implies that the tail of the distribution for GOE behaves as $\tau^{-M/2-2}$. In particular, for $M = 3$ we obtain for the time delay distribution $P(\tau) \approx \tau^{-7/2}$, in full agreement with the experimental finding in [26].

Similar numerical tests may also be performed for the velocity distribution in the case of a parametric dependence in order to test the formulas (2.19) and (2.20). To this end we have to introduce a parametric dependence into the basic model of Eqs. (1.2)–(1.3). One can, in principle, discuss several possible cases, the parameter x may affect either the bound system only [described by H_{kl} in Eq. (1.3)] or the decay part, i.e., the bound-continuum coupling W, or both. In a generic case, arguably, both parts of the effective Hamiltonian will be affected. We consider the case when the internal dynamics only is x dependent, i.e., $H = H(x)$. This situation corresponds directly to predictions obtained in the preceding section. A similar approach has been adopted in the treatment of time reversal symmetry-breaking influence on the conductance fluctuations [21].

The parametric x dependence is taken in a generic form: $H = H_1 \cos(x) + H_2 \sin(x)$ [18], where H_i are drawn indepen-
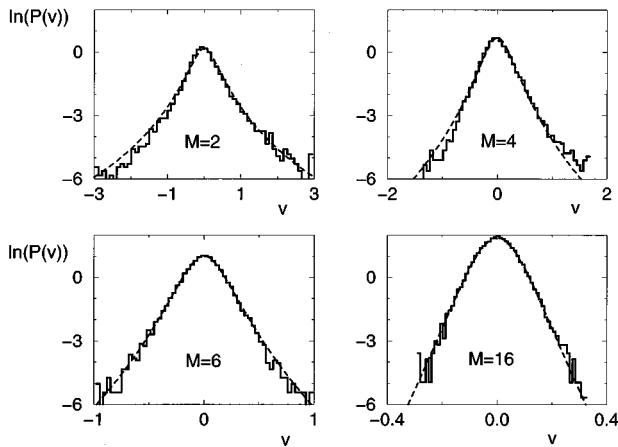
FIG. 6. Numerical data for distribution of slopes (with respect to external parameter) for GUE internal dynamic and $g = 1$ plotted in the semilogarithmic scale. The theoretical prediction Eq. (2.20) is shown as a full line and the number of channels is indicated in each graph. Note the strongly non-Gaussian shape of the distribution.
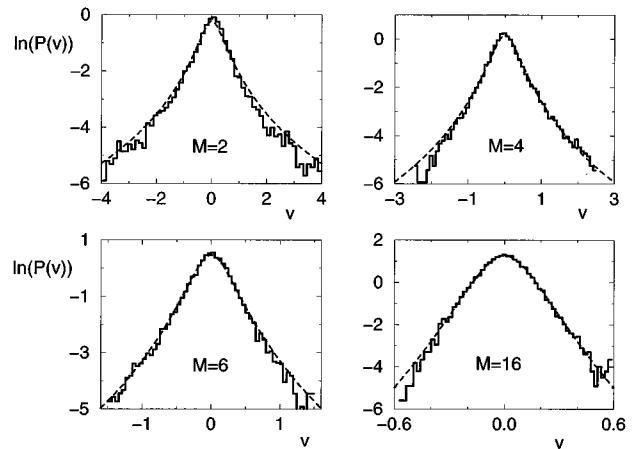

FIG. 7. Same as in the previous figure but for GOE internal dynamic. The theoretical prediction is obtained by the modification of Eq. (2.20) discussed in the text.

dently from the *same* ensemble of random matrices. The trigonometric form assures that the mean density of states remains the same for all x and the motion of bound levels as a function of x is stationary [18]. The slopes have been calculated by a finite difference in x from eigenphases of S. As before, more than 15 000 S matrices were used for the averaging.

In the GUE case the agreement between the numerical data and the analytic prediction for the slope distribution, Eq. (2.20), is again remarkable—see Fig. 6. Note strongly non-Gaussian character of the obtained distribution. In the semilogarithmic scale used in Fig. 6 a Gaussian would take an inverted parabola shape. The distributions show an algebraic tail $P(v) \propto v^{-(M+2)}$ for small M. For M large a center of the distribution resembles a parabola (i.e., a Gaussian distribution in the linear scale) followed by a straight line in the semilogarithmic plot indicating a regime of exponential behavior, $P(v) \propto \exp(-\gamma|v|)$. The numerical data are insufficient to detect a transition to a possible algebraic tail for $|v|$ large. For M even larger (not shown) the regime of Gaussian behavior broadens and the exponential behavior moves to the tails indicating the transition to the semiclassical limit.

Consider now GOE internal dynamics. Similarly as for the time delays, the agreement with the numerical data is admirable if the distribution (2.19) is evaluated with the "ad-hoc" improved $\widetilde{P}(\tau)$ given by Eq. (3.1)—compare Fig. 7. As before, the "proper" $P(\tau)$ [Eq. (2.12)] with $\beta = 1$ used in arriving at Eq. (2.20) leads to a theoretical prediction with clear disagreement with the numerical data for small M (not shown). The corrected expression is obtained from Eq. (2.20) by $\beta = 1$ and $M \rightarrow M + 1$ substitutions. The distributions obtained are similar in shape to those corresponding to the GUE case, with the algebraic tail of the form $P(v) \propto v^{-M/2-2}$ seen clearly for M small. For the largest number of channels plotted, $M = 16$, we again observe the Gaussian center with exponential tails in similarity with the GUE distribution.

To complete the discussion of the parametric dependence in the Hamiltonian based approach let us pass now to the curvature distributions. Numerical tests performed for the curvatures $K = d^2 s/dE^2$ are presented in Fig. 8. Note the quite good agreement of the numerical data with the generalized Cauchy distribution [18]. The double-logarithmic scale used enhances the small and large $|K|$ behavior. For large $|K|$ the agreement is excellent, confirming the universality of the large curvature tail behavior also for the present scattering system. On the other hand, one observes a slight excess of small curvatures (and the corresponding lack of "medium" curvatures). It is a clear indication that $M = 16$ is not sufficient to realize fully the semiclassical limit. Using the analogy with the bound system level dynamics [18] one may conclude that avoided crossings between eigenphases (as a function of the energy, E) are still partially isolated.

The curvature distribution with respect to the external parameter is plotted in Fig. 9. Comparing to the previous case, a better agreement with the generalized Cauchy distribution is observed, indicating that the semiclassical regime is reached faster when the motion of eigenphases as a function of x is considered. A similar qualitative conclusion may be reached considering the distribution of time delays and of the slopes with respect to the parameter x.

For M smaller one observes stronger deviations from the universal Cauchy distribution (not shown). The explicit dependence on the number of open channels in that case has obviously the same origin as the corresponding dependence in the case of slope (or time delay) distributions.

IV. RANDOM PARAMETRIC S MATRIX

As mentioned in the Introduction one often employs random ensembles to directly model properties of S matrices [10,12,13]. One may envision a similar approach for the study of the parametric statistics. To this end one has to define the parametric dependence of S matrices directly, without reference to the underlying bounded dynamics. Obviously, there is some ambiguity here, there are several possible choices. The ideal approach should be conceptually
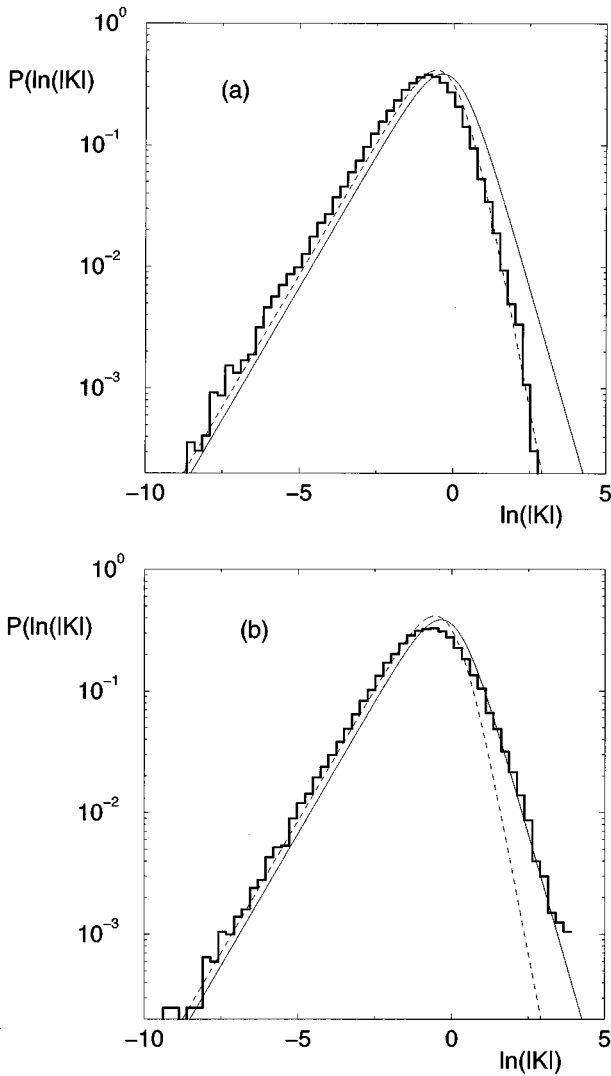
FIG. 8. Distribution of second derivatives of eigenphases of S matrix with respect to energy, $K = d^2 s / dE^2$ obtained numerically for the case of $M = 16$ open channels, (a) for GUE internal dynamics, (b) for GOE dynamics. The solid (dashed) lines in both panels represent the generalized Cauchy distributions corresponding to the GOE (GUE) case, respectively.

simple and, at the same time, lead to the same distributions as those obtained for the Hamiltonian based approach. After all, in both cases the parameter independent matrices belong to generalized circular ensembles [9]. We shall see below that the simplest possibilities agree with the Hamiltonian approach in the limit of a large number of channels (semiclassical limit) only.

The first approach proposed takes S matrices in the form

$$S(x) = S_0 \exp(ixV), \qquad (4.1)$$

where S_0 is drawn from the appropriate circular ensemble (COE or CUE) of a given rank M while V is a Hermitian matrix (rank M), independent of S_0 and drawn from GOE or GUE, respectively. Then the eigenphases at $x = 0$ are the phase shifts of S_0. The slopes and curvatures of S are easily defined as the corresponding derivatives at $x = 0$.
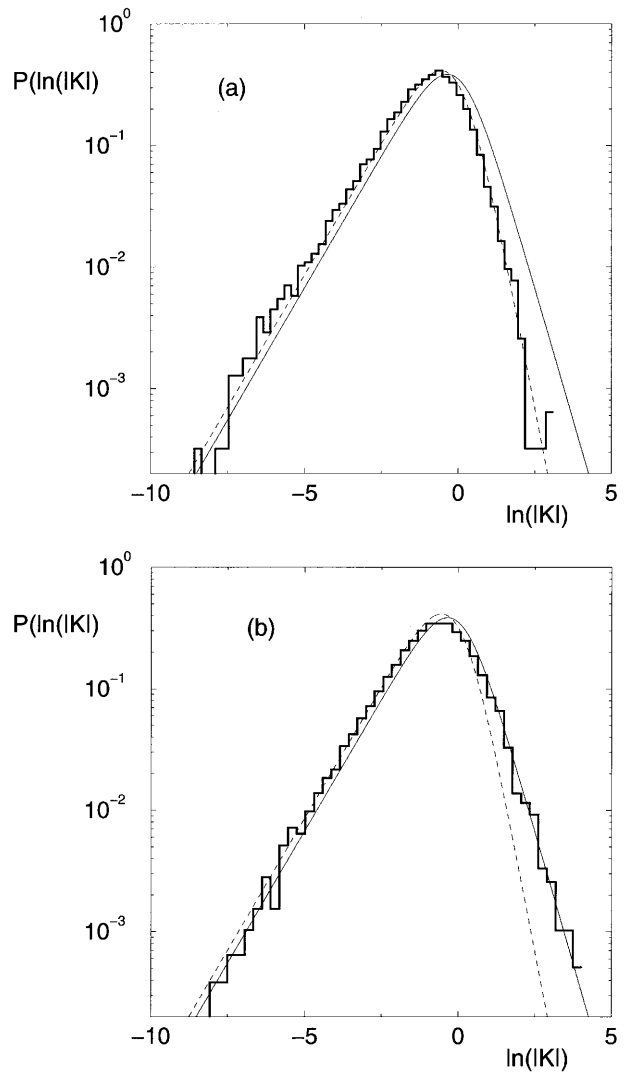

FIG. 9. As in the previous figure for the curvature with respect to an external parameter, $K = d^2 s / dx^2$.

Such a form of a parametric dependence is "borrowed" from the typical form of a Floquet operator corresponding to quantum maps (e.g., for a famous kicked rotator or for the kicked top—for a detailed introduction to such problems see [27]). While in [28] the form of the Floquet operator was determined by the dynamics of the system, here we assume a random S_0, as discussed above.

Equation (4.1) implies a Gaussian distribution of slopes, since the slopes of eigenphases of S at $x = 0$ are given by diagonal elements of matrix V represented in the eigenbasis of S_0. The latter are Gaussian distributed as we have taken S_0 and V independently. The Gaussian character of the velocity distribution for the model (4.1) is independent on the matrix size M and holds for both COE and CUE. Recalling the results obtained in the Hamiltonian model we see that the statistical predictions for eigenphase slope distribution coincide only in the $M \rightarrow \infty$ limit.

The random S matrices belonging to a given ensemble of random unitary matrices (COE, CUE) may be generated (for arbitrary M) by drawing the generalized Euler angles from the appropriate probability distribution [29]. Similarly one may construct the way to introduce the parametric depen-
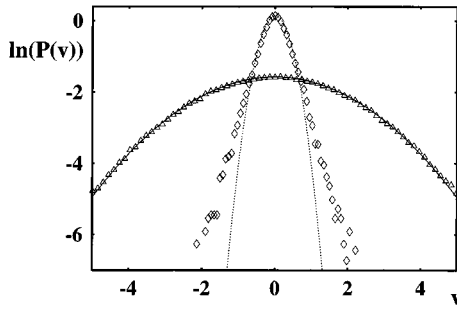
FIG. 10. Distribution of slopes of eigenphases with respect to the perturbation parameter x of random unitary matrices of size $M=40$ typical of COE; (a) parameter x controls variations of all M^2-1 Euler angles ($\triangle$); (b) only M diagonal angles are varied ($\diamond$). Solid and dotted lines represent Gaussian distributions (parabolas in the semilogarithmic plot) with the variance fitted to the center of the slope distributions.

dence by considering the infinitesimal changes of the generalized Euler angles [30]. Our numerical results indicate that if one assumes that *all* M^2-1 angles are affected by the perturbation in a same way, the distribution of slopes is *Gaussian* for arbitrary M.

Results received of 10^4 random unitary COE matrices with $M=40$ are presented in Fig. 10. Gaussian character of the ''velocity'' distribution, obtained in this case, is not at all typical of any parametric dynamics defined for random unitary matrices. On the contrary, one may construct many kinds of parametric dynamics in the space of unitary matrices leading to *non-Gaussian* distributions $P(v)$. Exemplary data, represented in the figure by triangles, were obtained for a model in which only M diagonal Euler angles have been varied. For small M the distributions obtained are closer to the results of the Hamiltonian model (1.2) than the pure Gaussian distribution. Similar results hold also for the CUE case.

Let us consider now the second derivatives of eigenphases with respect to x. For a Floquet operator corresponding to the kicked top model, the parametric curvature distribution has been studied already [28] and shown [18] to obey the generalized Cauchy distribution with quite a good accuracy for all three universality classes. The numerical simulations performed by us indicate that for M large (semiclassical limit) the same property holds for the S matrix models described above.

The simple propositions discussed above failed to reproduce the distribution of slopes with respect to the external parameter, x, obtained for small M within the Hamiltonian S-matrix model. However, this goal may be simply obtained by a slight modification of the assumption concerning the matrix V in Eq. (4.1). As discussed above, the distribution of slopes of S-matrix eigenphases is equivalent to the distribution of diagonal elements of V in the eigenbasis of S_0. Instead of choosing V to belong to the appropriate Gaussian random ensemble for the given symmetry, one may choose V from the ensemble defined by the desired distribution of diagonal elements, Eq. (2.19). This defines the distribution of M elements of V leaving the remaining $M(M-1)/2$ elements undefined (in a chosen basis). This additional freedom may be utilized to make this ensemble less artificial than

it seems at first. While this *a posteriori* procedure may be hardly described as an elegant one, it gives an indication of the properties of the required ensemble of V matrices. In particular, following the discussion presented in Sec. II, it is clear that the construction of such an ensemble may involve scalar products of unnormalized vectors in M-dimensional space [compare Eq. (2.10)]. Hopefully one may define the random ensemble for S matrices of the form (4.1) which is universal, i.e., reproduces not only the distribution of slopes but also of all other statistical measures involving the parameter x. This would allow us to use the ''direct'' S matrix approach instead of the Hamiltonian one, also for the problems involving the external parametric dependence.

V. CONCLUDING REMARKS

In this work we have considered the statistical properties of derivatives of the S matrix eigenphases with respect to the energy E as well as with respect to some external parameter x. Within the Hamiltonian approach we were able to derive, using simple heuristic arguments, the analytic distributions for the time delay valid for an arbitrary number of open channels M and an arbitrary value of the coupling constant g. An analytic distribution of slopes with respect to an external parameter has also been obtained. A comparison with the numerical simulations has shown good agreement of the theory with the numerical data in the CUE case. The discrepancies observed for the COE case may be removed by an *ad-hoc* modification of the proposed expression.

When the main part of this work was finished we were informed that in the CUE case the same formulas for the time delay distribution were obtained by Fyodorov and Sommers using supersymmetry calculus [31]. We hope that in the future the supersymmetric approach will be able to verify the proposed distributions also for the time-reversal invariant (COE) model.

We have verified numerically that the curvature distribution (i.e., the distribution of second derivatives of eigenphases with respect to energy) obeys the generalized Cauchy distribution [18] in the semiclassical limit (M large).

Construction of the parametric dependence directly for the random S matrices belonging to a given random ensemble has been shown to be ambiguous. The natural choices for the dynamics lead to Gaussian velocity distribution for an arbitrary number of open channels. Then the agreement with the Hamiltonian based approach is obtained in the $M\to\infty$ limit only.

[1] U. Smilansky, in *Chaos and Quantum Physics*, edited by M.-J. Giannoni, A. Voros, and J. Zinn-Justin, Les Houches Summer School, Session LII (North-Holland, Amsterdam, 1991).

[2] C. H. Lewenkopf and H. A. Weidenmüller, Ann. Phys. (N.Y.) **212**, 53 (1991).

[3] C. Mahaux and H. A. Weidenmüller, *Shell-Model Approach to Nuclear Reactions* (North-Holland, New York, 1969).

[4] J. J. M. Verbaarschot, H. A. Weidenmüller, and M. R. Zirnbauer, Phys. Rep. **129**, 367 (1985).

[5] C. M. Marcus, A. J. Rimberg, R. M. Westervelt, P. F. Hopkins, and A. C. Gossard, Phys. Rev. Lett. **69**, 506 (1992).

[6] A. M. Chang, H. U. Barnager, L. N. Pfeiffer, and K. W. West, Phys. Rev. Lett. **73**, 2111 (1994).

[7] O. Bohigas, in *Chaos and Quantum Physics* (Ref. [1]).

[8] M. L. Mehta, *Random Matrices*, II ed. (Academic, New York, 1991).

[9] P. W. Brouwer, Phys. Rev. B **51**, 16 878 (1995).

[10] P. A. Mello, P. Pereyra, and T. H. Seligman, Ann. Phys. (N.Y.) **161**, 254 (1985).

[11] F. J. Dyson, J. Math. Phys. **3**, 140 (1962).

[12] Y. Imry, Europhys. Lett. **1**, 249 (1986).

[13] K. A. Muttalib, J.-L. Pichard, and A. D. Stone, Phys. Rev. Lett. **59**, 2475 (1987).

[14] B. L. Altschuler and B. Shklovskii, Zh. Éksp. Teor. Fiz. **91**, 220 (1986) [Sov. Phys. JETP **64**, 127 (1986)]; P. A. Lee, D. Stone, and H. Fukuyama, Phys. Rev. B **35**, 1039 (1987); for a review see, e.g., *Mesoscopic Phenomena in Solids*, edited by B. L. Altshuler, P. A. Lee, and R. A. Webb (North-Holland, New York, 1991).

[15] R. A. Jalabert and J.-L. Pichard, J. Phys. I France **5**, 287 (1995).

[16] P. Gaspard, S. A. Rice, and K. Nakamura, Phys. Rev. Lett. **63**, 930 (1989); P. Gaspard, S. A. Rice, H. J. Mikeska, and K. Nakamura, Phys. Rev. A **42**, 4015 (1990).

[17] B. D. Simons and B. L. Altshuler, Phys. Rev. Lett. **70**, 4063 (1993); Phys. Rev. B **48**, 5422 (1993).

[18] J. Zakrzewski and D. Delande, Phys. Rev. E **47**, 1650 (1993).

[19] F. von Oppen, Phys. Rev. Lett. **73**, 798 (1994).

[20] A. M. S. Macedo, Phys. Rev. E **50**, R659 (1994).

[21] Z. Pluhař, H. A. Weidenmüller, J. A. Zuk, and C. H. Lewenkopf, Phys. Rev. Lett. **73**, 2115 (1994).

[22] E. Doron, U. Smilanski, and A. Frenkel, Physica D **50**, 367 (1991).

[23] E. Doron and U. Smilansky, Nucl. Phys. A **545**, 455c (1992).

[24] J. Spanier and K. B. Oldham, *An Atlas of Functions* (Hemisphere Publishing Corp., Washington, 1987).

[25] I. S. Gradshteyn and I. M. Ryzhik, *Tables of Integrals, Series and Products* (Academic, New York, 1980).

[26] H. Alt *et al.*, Phys. Rev. Lett. **74**, 62 (1995).

[27] F. Haake, *Quantum Signatures of Chaos* (Springer, Berlin, 1991).

[28] D. Saher, F. Haake, and P. Gaspard, Phys. Rev. A **44**, 7841 (1991).

[29] K. Życzkowski and M. Kuś, J. Phys. A **27**, 4235 (1994).

[30] K. Życzkowski and M. Kuś, Phys. Rev. E **53**, 319 (1996).

[31] Y. Fyodorov and H. J. Sommers, Phys. Rev. Lett. **76**, 9709 (1986).